Published in final edited form as:

ACS Nano. 2019 May 28; 13(5): 5720–5730. doi:10.1021/acsnano.9b01154.

Copper Sulfide Facilitates Hepatobiliary Clearance of Gold Nanoparticles through the Copper-Transporting ATPase ATP7B

Xiaodong Wang[#‡], **Liangran Guo**[#‡], **Sihang Zhang**[#†], **Yuan Chen**[#‡], **Yi-Tzai Chen**[‡], **Binbin Zheng**[†], **Jingwen Sun**[†], **Yuyi Qian**[†], **Yixin Chen**[‡], **Bingfang Yan**[‡,§], **Wei Lu**[*,†,‡]

[†]Key Laboratory of Smart Drug Delivery, Ministry of Education, & State Key Laboratory of Molecular Engineering of Polymers, School of Pharmacy & Minhang Hospital, Fudan University, Shanghai 201203, China

[‡]Department of Biomedical and Pharmaceutical Sciences, College of Pharmacy, The University of Rhode Island, Kingston, Rhode Island 02881, United States

[§]James L. Winkle College of Pharmacy, University of Cincinnati, Cincinnati, Ohio 45221, United States

[#] These authors contributed equally to this work.

Abstract

Metallic gold (Au) nanoparticles have great potential for a wide variety of biomedical applications. Yet, slow clearance of Au nanoparticles significantly hinders their clinical translation. Herein, we describe a strategy of utilizing the endogenous copper (Cu) clearance to improve the elimination of Au nanoparticles. Our mechanistic study reveals that a Cu-transporting P-type ATPase, ATP7B, mediates the exocytosis of CuS nanoparticles into bile canaliculi for their rapid hepatobiliary excretion. The efflux of CuS nanoparticles is adopted to facilitate the hepatobiliary clearance of Au nanoparticles through CuS–Au conjugation. Using two different CuS–Au nanoconjugates, we demonstrate that CuS increases the biliary Au excretion of CuS–Au nanospheres or CuS–Au nanorods in mice or rats in comparison to that of their respective unconjugated Au nanoparticles postintravenous injection. The current CuS–Au conjugation approach provides a feasible strategy to enhance the hepatobiliary clearance of Au nanoparticles that may be applicable to various structures.

Graphical Abstract

[*]**Corresponding Author**: Phone: +86-21-51980185. wlu@fudan.edu.cn.

ASSOCIATED CONTENT

Supporting Information

The Supporting Information is available free of charge on the ACSPublicationswebsite at DOI: 10.1021/acsnano.9b01154. TEM/EDS analysis of CuS nanoparticles in bile, TEM images of PEG-HCuSNPs in hepatocytes from mice at 4 or 24 h following the injection, characterization, and dissociation of PEG-HCuSNPs, STEM/EDX and dissociation analysis of PEG-HCuSNPs@Au in FBS, mRNA expression of *Atp7b* in mouse primary hepatocytes, normalized cellular Cu (%) following incubation with PEG-HCuSNPs, Western blot analysis of ATP7B, TEM images of PEG-HCuSNPs@Au, PEG-AuNPs, PEG-AuNRs, or PEG-SCuSNPs, STEM/EDX of PEG-HCuSNPs@Au in bile, TEM/EDS of PEG-HCuSNPs@ Au in hepatocytes from mice at 1 h following injection, immunofluorescence staining of the primarily cultured Kupffer cells, Au uptake and exocytosis profile of the nanoparticles by mouse Kupffer cells (PDF)

The authors declare no competing financial interest.

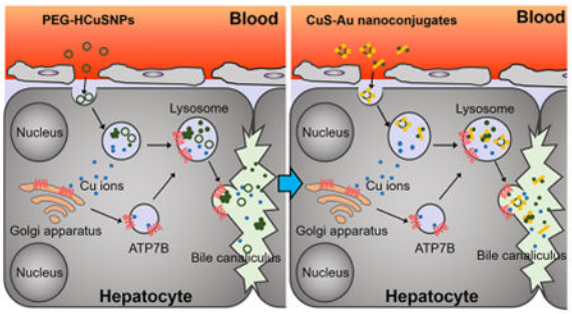

Keywords

copper sulfide nanoparticle; gold nanoparticle; hepatobiliary excretion; ATP7B; nanoconjugate

The intriguing optical and physicochemical properties of gold (Au) nanostructures endow them with great potential in biomedical applications.[1–3] Despite bioinert properties and biocompatibility of metallic Au nano-particles, the extremely long elimination half-lives limit their clinical translation.[4–7] To date, no effective strategies exist that enhance the metabolism and clearance of Au nanoparticles *in vivo*.

Our previous pharmacokinetic analyses have demonstrated that copper sulfide (CuS) nanoparticles are metabolizable.[8] The PEGylated hollow CuS nanoparticles (PEG-HCuSNPs) undergo excretion from the liver (67%ID, percentage of injected dose) and kidney (23%ID) within 1 month postinjection.[8] Liver is the major organ eliminating CuS nanoparticles. However, the process of hepatobiliary excretion of CuS nanoparticles remains unknown.

In this work, we use PEG-HCuSNPs to investigate the trafficking of CuS nanoparticles in hepatocytes and demonstrate that the rapid excretion of PEG-HCuSNPs is associated with the P-type ATPase copper (Cu) transporter ATP7B-mediated exocytosis into bile canaliculi. In light of this endogenous mechanism, we hypothesize that the ATP7B-mediated hepatobiliary excretion of CuS nanoparticles enhances the clearance of Au nanoparticles through CuS–Au conjugation (Scheme 1). By designing two different CuS–Au nanoconjugates, we demonstrate that the ~80 nm sized HCuSNPs enhance the biliary excretion of the ~40 nm sized Au nanospheres, and the ~5 nm sized CuS nanoparticles increase the biliary clearance of Au nanorods (~40 nmin length, ~10 nm in width) in mice.

RESULTS AND DISCUSSION

Fast Hepatobiliary Excretion of PEG-HCuSNPs through Efficient Nanoparticle Trafficking to Bile Canaliculi.

To understand how PEG-HCuSNPs were eliminated from the liver, we first collected bile samples from gallbladders at different times following intravenous (i.v.) injection of the nanoparticles in BALB/c mice. Transmission electron microscopy (TEM) illustrated that the nanoparticles appeared in bile as early as 15 min after the administration (Figures 1A and S1). Bile samples collected at 1 h, 4 h, 1 day, or 2 day postinjection contained both large and

small CuS nanoparticles, as confirmed by an energy-dispersive spectrum (EDS) analysis (Figure S1), suggesting that PEG-HCuSNPs broke down during the process of hepatobiliary excretion. We next centrifuged the bile samples to separate the pellet (large and small CuS nanoparticles) from the supernatant (Cu ions) for quantitative analysis of Cu. Figure 1B delineated a continuous hepatobiliary excretion of Cu in both particulate and ionic forms following i.v. injection of PEG-HCuSNPs. Excretion of CuS particles in gallbladders decreased over time, possibly attributed to the decreased concentration of the CuS nanoparticles in blood circulation. In comparison, biliary excretion of Cu ions remained relatively steady.

We looked further into the nanoparticle distribution in mouse hepatocytes *in vivo*. At 1 h postinjection, PEG-HCuSNPs were observed in the endolysosomes of hepatocytes, in which the hollow structures of the nanoparticles were maintained (Figure 2A, green arrowheads). Additionally, a number of CuS nanoparticles appeared in electron-dense structures (Figure 2B–E, orange arrowheads), whereas the others partially disintegrated (Figure 2C,D,F, blue arrowheads). EDS analysis confirmed that these structures consisted of Cu and S elements (Figure 2E–H). Noticeably, some CuS nanoparticles were found in the lysosome close to bile canaliculus (Figure 2I, the structure pseudocolored in light cyan), indicating that the nanoparticle-loaded lysosome was moving toward the apical membrane of the hepatocyte for exocytosis. This hypothesis was evidenced by the observation of CuS nanoparticles in bile canaliculus (Figure 2J). Slimilar trafficking of PEG-HCuSNPs was observed in hepatocytes of mice at 4 or 24 h postinjection (Figures S2 and S3). These results, correlating with the biliary distribution of Cu, evidenced that the injected PEG-HCuSNPs underwent fast endocytosis, and some nanoparticles disintegrated in the endolysosomal compartments of hepatocytes, followed by quick exocytosis into bile canaliculi for efficient hepatobiliary excretion.

The swift disintegration of PEG-HCuSNPs may be ascribed to the interaction between the nanoparticles and cellular ingredients, facilitating dissociation of Cu ions. As shown in Figure S4A, minimal Cu^{2+} dissociated from PEG-HCuSNPs in phosphate buffered saline (PBS) due to the extremely low solubility of CuS ($K_{sp} = 7.9 \times 10^{-37}$ at 25 °C).[9] Medium at lysosomal pH (pH 4.9)[9] only increased the released Cu ions to 3.6 and 9.7% of the totally fed Cu at 24 h and 7 days, respectively. Addition of amino acids to the medium, however, increased the Cu^{2+} release more significantly (Figure S4B), owing to the formation of copper/amino acid complexes.[10] In addition, glutathione (GSH) or metallothionine, considered part of the Cu storage system,[11] enhanced Cu ion dissolution, resulting in collapse and dissociation of PEG-HCuSNPs (Figure S4C–E, arrowheads). These findings indicated that cellular ingredients, such as amino acids and Cu storage systems, interacted with PEG-HCuSNPs to facilitate their dissociation and further release of Cu ions. However, the highest amount of released Cu^{2+} was induced by GSH, which was only about 20% at 24 h. The acidic condition at the lysosomal pH affected Cu dissociation but to a much lesser extent.

Trafficking and Expression of ATP7B in Hepatocytes for Cu Extrusion in Response to the Injected PEG-HCuSNPs.

Cu-transporting ATPase ATP7B, highly expressed in hepatocytes, is crucial for maintaining Cu homeostasis.[12] Under basal conditions, it transports Cu into the trans-Golgi network (TGN) for metalation of many essential cuproenzymes or ceruloplasmin. Acute increase of intracellular copper, on the other hand, triggers ATP7B-dependent Cu sequestration and excretion. ATP7B accumulates Cu and redistributes from TGN to late endosome/lysosome compartments, followed by fusion with the apical plasma membrane to extrude Cu ions into bile canaliculi.[12–14] To evaluate if ATP7B participated in the exocytosis of CuS nanoparticles, we primarily cultured hepatocytes from mice.[8] The primary culture had ~95% purity through immunostaining with the hepatocyte marker, cytokeratin 18 (Figure 3A). For confirmation of bile canaliculi formed in the cell culture, the hepatocytes were incubated with 5-(and-6)-carboxy-2′,7′-dichlorofluorescein diacetate (CDFDA). CDFDA can passively enter the cytoplasm of hepatocytes, where esterases metabolize it to a fluorescent product 5-(and-6)-carboxy-2′,7′-dichlorofluorescein (CDF).[15] CDF is the probe of multi-drug-resistant protein 2 and can only be excreted into the bile canaliculi by functional hepatocytes.[16] Figure 3B illustrates significant excretion of CDF by the hepatocytes cultured for 2 days. In addition, these cells expressed ATP7B (Figure 3C). These results validated the function maintained in the primarily cultured mouse hepatocytes.

Fluorescence imaging confirmed that rhodamine isothiocyanate (RITC)-conjugated PEG-HCuSNPs (PEG-HCuSNPs-RITC) were effectively excreted into bile canaliculi by the hepatocytes (Figure 3D, arrow). Without PEG-HCuSNPs, ATP7B resided at perinuclear sites (Figure 3C, arrowheads). In the presence of fluorescein isothiocyanate (FITC)-conjugated PEG-HCuSNPs (PEG-HCuSNPs-FITC), some ATP7B was relocated in the cytoplasm membrane between the two cells (Figure 3E, arrowheads). More importantly, ATP7B fused with the nanoparticles in the bile canaliculi (Figure 3E, arrow). To further confirm the ATP7B-mediated exocytosis of CuS nanoparticles, we knocked down the cellular expression of *Atp7b* to below 20% of the normal level in the mouse hepatocytes by the siRNA–lipoplex (Figure S5A). We then cultured the mouse hepatocytes in Transwell and incubated the cells with PEG-HCuSNPs. After incubation with the nanoparticles for 30 min, the cellular content of Cu particles in the *Atp7b*-downregulated hepatocytes was 4.63-fold as high as that in the normal hepatocytes (Figure 3F). This was possibly attributed to the enhanced cellular retention of the Cu nanoparticles through the inhibition of ATP7B-mediated exocytosis. Replaced with the fresh medium and incubated for another 30 min for exocytosis, a significantly higher cellular percentage of Cu particles remained in the *Atp7b*-down-regulated hepatocytes compared to that in the normal cells (Figure S5B), further indicating that ATP7B played a significant role in the exocytosis of the CuS particles.

The above results indicated that the quick hepatic excretion of PEG-HCuSNPs was associated with ATP7B. This was evidenced by the colocalization of the fluorescence of ATP7B with that of PEG-HCuSNPs-FITC and Rab7, a marker of late endosome/lysosome structures,[17] in hepatocytes of mice at 1 h postinjection (Figure 4A, arrows). We further isolated the hepatocytes from BALB/c mice following the injection of PEG-HCuSNPs for Western blot analysis. At 1 h postinjection, levels of ATP7B increased by 28% in cytosol

and by 72% on the plasma membrane of hepatocytes (Figure 4B,C). This finding denoted that the body quickly launched an endogenous detoxification machinery in hepatocytes in the presence of the PEG-HCuSNPs loading. Increase of ATP7B on the plasma membrane was substantially more than that in cytosol, indicating that more ATP7B migrated to the cell canalicular membrane in order to accelerate Cu excretion for homeostasis.[12,18] The expression of ATP7B decreased in cytosol at 4 or 24 h postinjection (Figure 4B,C) but restored to baseline at 2 days postinjection (Figure S6). One possible explanation was that the cellular storage of ATP7B was temporarily exhausted and production of ATP7B transiently did not meet the demand at the nanoparticle's dose of 20 mg/kg of Cu.

Western blot analysis further revealed that ATP7B bound to the CuS nanoparticles in hepatocytes postinjection (Figure 4D), suggesting that ATP7B participated in sequestering and chelating not only Cu ions but also Cu nanoparticles. Because of the slow release of Cu ions from CuS nanoparticles in the acidic lysosome (Figure S4A), a significant amount of CuS nanoparticles remained undissociated (particulate Cu) in the endolysosomal compartment in hepatocytes (Figure 2 and Figures S2 and S3). It is also possible that the dissolved Cu ions could interact with salts to re-form Cu nanoparticles. The trafficking pathway of hepatobiliary excretion of PEG-HCuSNPs could be as follows. Following i.v. injection of PEG-HCuSNPs and uptake by the hepatocytes, PEG-HCuSNPs either remain intact or break down into smaller CuS nanoparticles partially or completely in the endolysosomal compartments. Cu ions are dissociated in the endocytic vesicles during the nanoparticle's disintegration. Some Cu ions were further released into cytosol. Others may re-form Cu particles in the endolysosomes. Cu-ATPase ATP7B chelates the cytosolic Cu ions and redistributes from TGN to late endosome/lysosome compartments where ATP7B fuses with the apical plasma membrane to extrude Cu ions into bile canaliculi. Moreover, ATP7B traverses the Cu-particle-loaded vesicles participating in removal of intravesicular Cu through chelating both ionic and particulate Cu (Scheme 1).

CuS Facilitates Hepatobiliary Clearance of Gold Nanoparticles through CuS–Au Conjugation.

To prove if CuS facilitates the hepatobiliary elimination of Au nanoparticles, we first synthesized Au nanoparticles (AuNPs) on the surface of HCuSNPs. The synthesized PEG-HCuSNPs@Au with ~40 nm diameter Au nanospheres had a Au/Cu ratio of ~5:1 (w/w) (Figures 5A and S7A). Energy-dispersive X-ray spectroscopy (EDX) confirmed the distribution of Au or Cu in PEG-HCuSNPs@Au (Figure 5A). For comparison, ~40 nm diameter Au nanospheres were synthesized (Figure S7B). The fluorescence image depicts RITC-labeled PEG-HCuSNPs@Au (PEG-HCuSNPs@Au-RITC) colocalized with CDF in bile canaliculi (Figure 5B, top row, arrows), whereas RITC-labeled PEGylated AuNPs (PEG-AuNPs-RITC) colocalized with CDF in intracellular vesicles at perinuclear sites (Figure 5B, bottom row, arrowheads). Further, PEG-HCuSNPs@Au-RITC but not PEG-AuNPs-RITC colocalized with ATP7B in bile canaliculi (Figure 5C, arrow). We next quantitatively analyzed the cellular excretion of the two nanoparticles by the mouse hepatocytes in Transwell. The cells were incubated with the nanoparticles for 5 min of uptake, followed by the replacement with fresh medium for exocytosis. Within 30 or 60 min of exocytosis, significant excretion of Au in the PEG-HCuSNPs@Au group was observed in

comparison with that in the PEG-AuNPs group (Figure 5D, left). In the plated human primary hepatocytes, PEG-HCuSNPs@Au enhanced the excretion of Au within 10 or 60 min of the exocytosis compared to that with PEG-AuNPs (Figure 5D, right). Knockdown of *Atp7b* in mouse hepatocytes significantly reduced the excretion of PEG-HCuSNPs@Au within 30 or 60 min of exocytosis, whereas the excretion was not decreased in the hepatocytes transfected with scrambled siRNA in comparison with that in normal hepatocytes (Figure 5E, left). However, *Atp7b* knockdown in mouse hepatocytes did not change the exocytosis rate of PEG-AuNPs (Figure 5E, right). These data showed that HCuSNPs facilitated the exocytosis of AuNPs from hepatocytes through ATP7B-mediated Cu excretion.

Considerably, Au content in gallbladders from mice treated with PEG-HCuSNPs@Au was 28-fold as high as that in the PEG-AuNPs-treated mice at 4 h postinjection (Figure 5F). The structures of PEG-HCuSNPs@Au were observed in bile (Figures S8) and further confirmed in hepatocytes in the liver (Figure S9) of mice following the injection. In comparison with the PEG-AuNPs group, treatment with PEG-HCuSNPs@Au resulted in the increased Au excretion by 3.1-fold and 5.0-fold in the feces of the first day and the second day following the injection, respectively (Figure 5G). After 2 days, the results of Au excretion did not show significant difference between the two groups, possibly ascribed to the dissociation of Cu from Au particles *in vivo*. This was confirmed by STEM/EDX and dissolution analysis of PEG-HCuSNPs@Au in fetal bovine serum (FBS), showing the disintegration of the nanoconjugates and the dissociation of Cu from Au following the incubation (Figure S10). To further prove the facilitated hepatobiliary excretion of Au through CuS–Au conjugation, we continuously collected bile for 6 h from rats following the i.v. injection of PEG-HCuSNPs@Au or PEG-AuNPs. Figure 5H demonstrated that injection of PEG-HCuSNPs@Au increased the cumulative biliary excretion of Au by 2.13-fold in comparison with PEG-AuNPs in rats. These results collectively supported the significantly enhanced hepatobiliary excretion of AuNPs following conjugation with HCuSNPs.

We next synthesized small CuS nanoparticles (SCuSNPs) of ~5 nm in diameter that were conjugated to Au nanorods through HS-PEG_{5k}-COOH following N-hydroxysuccinimide activation to form PEG-AuNRs@CuS (Au/Cu = 2.9:1, w/w, Figures S11 and 6A). The fluorescence image revealed the colocalization of FITC-labeled PEG-AuNRs@CuS with ATP7B in bile canaliculi as early as 5 min following the incubation (Figure 6B, arrows). By contrast, PEG-AuNRs were mainly found in the intracellular vesicles during the whole 35 min incubation (Figure 6C, arrowheads). RITC-labeled PEG-AuNRs@CuS but not PEG-AuNRs colocalized with CDF, further confirming the biliary excretion of PEG-AuNRs@CuS (Figure 6D, arrow). PEG-AuNRs@CuS significantly enhanced the cellular excretion of Au in mouse hepatocytes within 10, 30, or 60 min of the exocytosis in comparison with the unconjugated PEG-AuNRs or the simple mixture of PEG-AuNRs and PEG-SCuSNPs with the same Au/Cu ratio as that of PEG-AuNRs@ CuS (Figure 6E, left). This result demonstrated the facilitated Au exocytosis through the conjugation of Au with CuS, whereas the co-incubation of the separated Au and CuS NPs remained ineffective. The accelerated Au excretion by PEG-AuNRs@CuS was also observed in human hepatocytes (Figure 6E, right). Downregulation of *Atp7b* in mouse hepatocytes significantly reduced the exocytosis rate of Au in the PEG-AuNRs@CuS-treated group but not in the PEG-AuNRs-

treated group (Figure 6F). The Au content in the gallbladder from the PEG-AuNRs@ CuS-treated mice was 2.68-fold as high as that in the PEG-AuNRs-treated mice at 4 h postinjection (Figure 6G). These results proved the increased exocytosis of AuNRs by hepatocytes through SCuSNPs coupling.

CONCLUSION

Our current findings revealed that the efficient hepatobiliary excretion of CuS nanoparticles is attributed to the participation of Cu-transporting ATPase ATP7B. Due to slow release of Cu ions from the endocytosed CuS nanoparticles, ATP7B traverses the endolysosomal compartment to chelate intravesicular Cu, regulating both ionic and particulate Cu excretion into bile canaliculi. On the basis of this mechanism, the accelerated hepatobiliary excretion of Au nanoparticles was achieved through either conjugation of Au nanospheres to the surface of CuS nanoparticles (PEG-HCuSNPs@Au) or coupling of small CuS nanoparticles to the surface of Au nanorods (PEG-AuNRs@CuS) (Scheme 1). The CuS–Au conjugation approach would provide a feasible strategy to accelerate the clearance of Au nanoparticles in various structures.

EXPERIMENTAL SECTION

Materials.

All chemicals used were purchased from Sigma-Aldrich Chemical, Inc. unless mentioned specifically. BALB/c mice (6–8 weeks, both male and female) were ordered from Charles River Laboratories International, Inc. or Sino-British Sippr/BK Lab Animal. All animal experiments were conducted in compliance with the guidelines for the care and use of research animals established by the University of Rhode Island Institutional Animal Care or Use Committee (IACUC) and Fudan University IACUC. Plated human primary hepatocytes (24-well plates) were obtained from the Liver Tissues Procurement and Distribution System (University of Pittsburgh).

Synthesis of HCuSNPs.

The HCuSNPs were synthesized according to our previously reported method.[8,19] The synthetic HCuSNPs were centrifuged at 11 000 rpm for 15 min at room temperature and washed twice with distilled water. HCuSNPs were then resuspended in 4.8 mL of water containing with 200 μL of methoxy-PEG_{5k}-SH (20 mg/mL, MW 5000, JenKem Technology) overnight at room temperature to obtain PEG-HCuSNPs. The nanoparticles were washed twice with distilled water and stored at 4 °C for future use.

Synthesis of AuNRs.

AuNRs were synthesized according to a two-step method.[20–22] The OD of the AuNRs solution was measured by the UV–vis spectrum, whose peak was around 750 nm. The length (~40 nm) and width (~10 nm) of the synthetic AuNRs were examined by TEM.

Synthesis of AuNPs.

Ten milligrams of chlorauric acid in 95 mL of solution was heated to the boiling point with stirring. One milliliter of sodium citrate solution (10 mg/mL) was then added to the boiling solution. After about a minute of stirring, the solution became very faint grayish-pink and then gradually darkened over a period of about 10 min. The final color of the solution was deep amaranth.[23]

Synthesis of PEG-HCuSNPs@Au.

PEG-HCuSNPs@Au were synthesized through a one-step method according to a previous publication with modification.[24] One milliliter of the above prepared HCuSNPs suspension was dispersed in 1.2 mL of 100% ethanol, followed by the addition of 10 mg of PVP-K30. After being stirred for 30 min, 9.6 mL of $HAuCl_4 \cdot 3H_2O$ aqueous solution (0.3 mM) was added. After being stirred for 10 min, the mixture was added with 0.5 mL of $NaBH_4$ (3 mM), and stirred for another 30 min. The products were collected by centrifugation at 11 000 rpm for 15 min and washed three times with 100% ethanol. HCuSNPs@Au were then resuspended in water and coated with methoxy-PEG_{5k}-SH as described above.

Synthesis of SCuSNPs.

In a 50 mL falcon tube, 9 mL of ddH_2O was added and stirred. The following reagents were added sequentially: 100 μL of $CuCl_2$ (100 mM), 50 μL of methoxy-PEG_{5k}-SH (5 mg), and 1 mL of glutathione (6.1 mg). The pH of the mixture was adjusted to pH 9.3 with NaOH. Then, the mixture was vented with argon for 5 min, followed by addition of 2 mL of thioacetamide (0.8 mg). Afterward, the mixture was kept in the water bath (50 °C) with magnetic stirring for 2 h. The synthesized SCuSNPs were concentrated using an ultracentrifuge tube (Amicon Ultra-15, cutoff MW 10 kD, EMD Millipore) in a swing bucket centrifuge (4000g) for 15 min. The concentrated nanoparticles were washed with ddH_2O.[25]

Synthesis of PEG-AuNRs@CuS.

The above prepared AuNRs (0.5 mg) were mixed with 1 mg of methoxy-PEG_{5k}-SH and 0.1 mg of SH-PEG_{5k}-COOH (Nanocs) in 1 mL of ddH_2O. Then, the mixture was sonicated for 10 min and left on the rotor plate at room temperature overnight. On the second day, PEG-AuNRs were activated with 0.4 mg of (3-dimethylaminopropyl)-*N*-ethylcarbodiimide hydrochloride (EDC·HCl) and 0.6 mg of *N*-hydroxysuccinimide for 1 h at room temperature. The activated PEG-AuNRs were centrifuged for 10 min at 14 000 rpm and washed with 0.1 M cold 2-morpholinoethanesulfonic acid twice. Then, the pellet was washed with 1 mL of PBS and centrifuged for 10 min at 14 000 rpm. AuNRs (1 mL) were added to 4 mL of the above freshly prepared SCuSNPs. After 15 min sonication, the mixture was placed on the rotor plate for 24 h at room temperature. The mixture was centrifuged at 11 000 rpm for 10 min to remove the unconjugated SCuSNPs. Then, the pellet was washed twice and stored at 4 °C in 100 μL of ddH_2O.

For FITC or RITC labeling of the above nanoparticles, methoxy-PEG_{5k}-SH was replaced with the same total amount of a mixture of methoxy-PEG_{5k}-SH and FITC-PEG_{5k}-SH (Nanocs) or RITC-PEG_{5k}-SH (Nanocs) at a mass ratio of 9:1.

Excretion of Nanoparticles into Gallbladders in Mice.

BALB/c mice were divided into 6 groups (n = 3–4). One group of mice injected with saline was used as a blank control. The other 5 groups received i.v. injection of PEG-HCuSNPs (20 mg/kg body weight of Cu). At 15 min, 1 h, 4 h, 24 h, or 2 days postinjection, the gallbladder of each mouse was collected. The content of each gallbladder was then centrifuged at 13 523g for 15 min to separate the pellet (CuS nanoparticles) and supernatant (Cu ions). The supernatant of each sample was directly added to a 2% nitric acid solution for inductively coupled plasma mass spectrometer (ICP-MS) analysis (model X7, Thermo Electron Corporation) of Cu. The pellet was added with nitric acid and digested by Mars 5 microwave system (CEM Corporation), 0.2 mL of which was added to 9.8 mL of deionized water for ICP-MS analysis. In a parallel study, the pellet was resuspended in water and directly deposited on the Formvar-coated nickel grid (200 mesh, Ted Pella, Inc.) without counterstaining. The grids were placed on a beryllium holder and analyzed with TEM (JEOL, JEM2100) and EDS (Oxford, INCA x-sight). For analysis of biliary Au content, mice were i.v. injected with PEG-HCuSNPs@Au (20 mg/kg of Au, 4 mg/kg of Cu), PEG-AuNPs (20 mg/kg of Au), PEG-AuNRs@CuS (20 mg/kg of Au, 6.9 mg/kg of Cu), and PEG-AuNRs (20 mg/kg of Au).

Analysis of Au in Feces.

BALB/c mice were divided into two groups housed in the metabolic cage (n = 4). Mice were allowed to adapt to the environment for 3 days. The feces during each day were collected as the blank. After three days, the mice were i.v. injected with PEG-AuNPs (20 mg/kg of Au) and PEG-HCuSNPs@Au (20 mg/kg of Au, 4 mg/kg of Cu). The feces were collected every day for another week. All of the samples were dried, weighed, and digested with aqua regia. The Au content was quantified by an inductively coupled plasma optical emission spectrometer (ICP-OES, iCAP 7400, Thermo Fisher Scientific).

Excretion of the Nanoparticles into Bile in Rats.

Sprague–Dawley rats (180–220 g, 4–6 weeks, male, Shanghai SLAC) were divided into two groups (n = 3). The rats were under anesthetic conditions during the surgical operation and the experiment. An indwelling needle was inserted into the bile duct for bile collection. After blank bile was collected for 15 min, the rats were i.v. injected with PEG-AuNPs (20 mg/kg of Au) and PEG-HCuSNPs@Au (20 mg/kg of Au, 4 mg/kg of Cu). The bile samples were collected at 0.25, 0.5, 0.75, 1, 1.5, 2, 4, or 6 h after the injection. All of the samples were digested with aqua regia, and the Au content was measured by ICP-OES.

Preparation of Liver Tissue Samples for TEM.

BALB/c mice were i.v. injected with PEG-HCuSNPs or PEG-HCuSNPs@Au (both 20 mg/kg of Cu). At predetermined time points, the mice were euthanized and the livers were quickly collected, cut into 1 mm^3, and fixed in the fixation reagent (2.5% glutaraldehyde plus 2% paraformaldehyde in 0.1 M of phosphate buffer, pH 7.4). The TEM sample preparation followed a routine procedure. The samples were embedded in Epon resin followed by ultrathin sectioning (60–70 nm thickness). The sections were placed on nickel grids with Formvar/carbon film stained with 7% uranyl acetate and lead citrate. The samples

were examined under a TEM microscope (FEI, Tecnai Biotwin, LaB6, 80 kV). For TEM/EDS analysis, the sections were directly deposited on molybdenum, nickel, or gold grids without postsection staining. The grids were placed on a beryllium holder and analyzed with TEM (FEI, Tecnai G^2 20 TWIN) and EDS (Oxford, EDX 6767).

Isolation of Primary Mouse Hepatocytes.

Primary mouse hepatocytes were isolated by a two-step collagenase perfusion.[8,26] After perfusion, the mouse liver was excised and finely broken into small pieces by forceps in washing buffer (Williams' Medium E with 1% of penicillin and streptomycin). The resulting cell suspension was passed through a 40 μm cell strainer to remove undigested tissue. The single-cell suspension was then obtained and transferred to a 50 mL conical tube for centrifugation (50*g*) for 5 min at 4 °C. The hepatocyte pellet was further purified with 100% Percoll (GE Healthcare). After being washed, the highly purified hepatocytes were resuspended in culture medium for future use.

For characterization of the hepatocytes, the freshly isolated hepatocytes were seeded in a chamber slide precoated with collagen (1 mg/mL). After 2 days, the cells were fixed with cold acetone for 5 min followed by blocking with 10% goat serum for 30 min at room temperature. The cells were incubated with rabbit anti-mouse cytokeratin 18 mAb (Abcam, 1:100) at 4 °C overnight. After being washed with PBS three times, the cells were stained with Alexa Fluor 555 goat anti-rabbit IgG (1:500, Thermo) for 1 h at room temperature. After being washed with PBS three times, the cell nuclei were counterstained with DAPI (5 μg/mL). For characterization of ATP7B, the hepatocytes cultured in the collagen-precoated 35 mm Petri dish were fixed with 4% paraformaldehyde, blocked with 10% of FBS, and stained with goat anit-ATP7B antibody (1:100, Santa Cruz Biotechnology) followed by Alexa Fluor 555-conjugated donkey antigoat IgG (1:500, Thermo). The cell nuclei were counterstained with DAPI (5 μg/mL).

For visualization of the colocalization ATP7B with the nanoparticles, the cells were incubated with 10 μg/mL of FITC-labeled PEG-HCuSNPs, PEG-HCuSNPs@Au, PEG-AuNPs, PEG-AuNRs, or PEG-AuNRs@CuS for different times, followed by fixation, ATP7B immunofluorescence staining, and DAPI counterstaining as described above.

CDFDA Assay.

For confirmation of function of bile canaliculi, the isolated mouse primary hepatocytes were seeded in a 35 mm Petri dish precoated with rat tail type I collagen (Corning) and cultured for 2 days. The cells were washed twice with 1 mL of prewarmed HBSS (with Ca^{2+}/Mg^{2+}). Then, 1 mL of prewarmed HBSS (with Ca^{2+}/Mg^{2+}) containing 5 μM of CDFDA was added and the cells incubated for 20 min in a 37 °C incubator with 5% CO_2. The cell nuclei were counterstained using Hoechst 33342 (1:1000). Washed with the prewarmed HBSS (with Ca^{2+}/Mg^{2+}) twice, the cells were directly visualized under Zeiss LSM 700 confocal microscope using a water immersion objective (Achroplan, 40×/0.80 W, WD = 3.6 mm, Carl Zeiss).

For visualization of the colocalization CDF with the nanoparticles, the cells were incubated with 10 μg/mL of RITC-labeled PEG-HCuSNPs, PEG-HCuSNPs@Au, PEG-AuNPs, PEG-

AuNRs, or PEG-AuNRs@CuS for 30 min, followed by CDFDA and Hoechst 33342 staining as described above.

Quantification of Cu or Au in Mouse Hepatocytes Following Incubation with Different Nanoparticles.

Transwells with a pore size of 3 μm (Corning) were coated with 50 μg/mL of type I collagen in 0.02 M glacial acetic acid for 1 h followed by PBS washing with a 4-fold volume. The Transwells were then coated with 1.5 mg/mL of type I collagen and incubated in the cell culture incubator for 15 min. Two days before the experiment, a single layer of hepatocytes was seeded with 500 and 1500 μL of cell culture medium (WME with 2% fresh mouse serum) fed to the upper compartment (apical) and the lower compartment (basolateral), respectively. For analysis of cellular Cu content, the apical medium was replaced with 500 μL of medium containing PEG-HCuSNPs (10 μg/mL of Cu) for 30 min at 37 °C. The apical medium was aspirated and quickly washed with 500 μL of prewarmed WME on both sides. Then, 100 μL of CelLytic M cell lysis reagent was added to the upper chamber, and cell lysate was transferred into a 1.5 mL Eppendorf tube. In parallel groups, following the nanoparticle incubation and washing, 500 μL of fresh cell culture medium was added to the upper compartment. The cell culture insert was transferred to another well with 1.5 mL of medium. After another 30, 60, or 90 min for exocytosis, the upper compartment medium was aspirated and washed with 500 μL of warm WME on both sides. Then, 100 μL CelLytic M cell lysis reagent was added to the upper compartment, and the cell lysate was transferred into a 1.5 mL Eppendorf tube. The collected cell lysates were centrifuged at 13 523g for 10 min, and the pellet was transferred for the ICP-MS analysis separately.

For the analysis of cellular uptake and exocytosis of CuS–Au conjugates in comparison with Au nanoparticles, the apical medium containing PEG-AuNPs, PEG-HCuSNPs@Au, PEG-AuNRs, PEG-AuNRs@CuS, or the mixture of PEG-AuNRs and PEG-SCuSNPs with the same Au/Cu ratio as that of PEG-AuNRs@CuS (10 μg/mL of Au in all groups) was added for 5 min of uptake at 37 °C. After being washed, fresh cell culture medium was added to the upper compartment. The cell culture insert was transferred to another well with 1.5 mL of fresh medium for exocytosis. At 5, 15, 35, or 65 min, the uptake or exocytosis experiment was terminated using the above-described method. The cell lysates were collected for analysis of cellular Au content and cellular protein.

The cell lysates were dissolved in 4 parts HNO_3 and 1 part HC1 overnight for digestion. Before the sample was loaded to ICP-MS for quantitative analysis of Cu or Au, the solvent was diluted to a mixture containing 2% HNO_3 and 2% HC1. The standards of Cu or Au were diluted into six concentrations (0.1, 0.25, 1, 25, 50, 100, and 250 ppb) and were run during analysis of the samples each time. The protein content of the cell lysates was analyzed by Pierce Coomassie (Bradford) protein assay kit (Thermo Fisher Scientific).

The % dose/mg protein represents the cellular Cu or Au content, which is calculated as follows:

$$\%\text{dose/mg protein} = \frac{\text{cellular Cu or Au (μg) per well}}{\text{Cu or Au added (μg) per well}} \Big/ \text{cellular protein (mg) per well} \times 100\% \quad (1)$$

For the excytosis study of CuS–Au conjugates, the decreased percentage of cellular Au content during the excytosis period from 0 to t min is designated as % Au exocytosis$_{0-t}$, which is calulcated as follows:

$$\%\text{Au exocytosis}_{0-t} = \left(1 - \frac{\%\text{ dose/mg of protein}_{t+5}}{\%\text{ dose/mg of protein}_5}\right) \times 100\% \quad (2)$$

where % dose/mg protein$_5$ represents the initial cellular Au content at 5 min following the uptake of the nanoparticles; % dose/mg protein$_{t+5}$ represents the cellular Au content remained at t + 5 min, which is the cellular Au content at 15, 35, or 65 min in this study.

Preparation of Membrane and Cytosol Fractions of Hepatocytes.

Membrane and cytoplasmic fractions from the perfused primary hepatocytes in mouse at different times following injection of PEG-HCuSNPs (20 mg/kg of Cu) were prepared as previously described with some modification.[27] Approximately 100 mg of mouse primary hepatocytes were lysed and homogenized in 900 μL of sucrose-Tris (pH 7.2) buffer containing 250 mM of sucrose, 1 mM of EDTA, 10 mM of Tris HCl, and protease inhibitors (100× Halt Protease and Phosphatase Inhibitor Cocktail, ThermoFisher). The homogenates were sonicated for three times (10 s per pulse, 30 s interval). The lysates received first centrifugation at 500g for 10 min to remove cellular debris. A second centrifugation at 6000g for 10 min was used to pellet the CuS nanoparticles. A third centrifugation at 100 000g for 60 min was applied to separate cytosolic fractions from the lysates. The pellets were then washed with 900 μL of sucrose-Tris buffer and centrifuged at 100 000g for 60 min. After being washed, the pellets were suspended with 50 μL of sequential extraction kit reagent 3 (Bio-Rad) and centrifuged at 100 000g for another 60 min. The resulting supernatant was membrane fractions. All experiments were conducted at 4 °C. The total protein concentrations of these samples were determined using Pierce 660 nm protein assay reagents (Thermo Fisher Scientific).

Western Blot Analysis.

Western blot was used to identify and semiquantify proteins of interest isolated from the above samples. Thirty micrograms of total protein premixed with Laemmli buffer (Bio-Rad) containing 0.1% β-mercaptoethanol was loaded per well for sodium dodecyl sulfate–polyacrylamide gel electrophoresis (Bio-Rad 4–20% Mini-PROTEAN TGX precast protein gel). The proteins were transblotted on Bio-Rad PVDF membrane at 120 V for ~70 min. After the transfer, the membrane was blocked for 2 h in 1× Tris-buffered saline with 0.1% Tween 20 (TBST) and 8% nonfat dry milk at room temperature. The membrane was then incubated with mouse anti-ATP7B monoclonal antibody (1:500, Santa Cruz) or mouse anti-β-actin monoclonal antibody (1:5000, Sigma) in TBST overnight at 4 °C. After being washed with TBST, the membrane was incubated with goat anti-mouse HRP secondary

antibody (1:10 000, Novex) for 1 h at room temperature. The membrane was then washed and incubated with an ECL fluorescence kit (Bio-Rad Clarity Western ECL Substrate) or SuperSignal West Femto maximum sensitivity substrate (Thermo Fisher Scientific). Membranes were exposed in Gel Logic 2200 Pro and were qualified with ImageQuant TL image analysis software (GE Healthcare). Levels of β-actin were used to normalize ATP7B expression in cytosol and membrane.

Statistical Analysis.

Statistical analysis was performed using GraphPad Prism 5 software. Data were presented as mean ± SD for all results. Statistical significance was determined either by analysis of variance (ANOVA) with Tukey's test for comparing means of multiple groups or by Student's t-test for two groups; $p < 0.05$ was considered significant.

Supplementary Material

Refer to Web version on PubMed Central for supplementary material.

ACKNOWLEDGMENTS

This work was partially supported by grants from the National Natural Science Foundation of China (81673018, 91859110) and the National Institutes of Health (R01EB018748, R01GM061988, and P20GM103430). The authors thank R. Kingsley from the University of Rhode Island for assisting in TEM of PEG-HCuSNPs in bile, C. Ayala from Rhode Island Hospital and X. Liu from Yale University Medical School for assisting in preparation and TEM of liver tissue samples with HCuSNPs, M. Rooks from Yale Institute of Nanoscience and Quantum Engineering for assisting in STEM/EDX, and G. Zhou from Fudan University for assisting in preparation and TEM/EDS analysis of liver tissue samples with PEG-HCuSNPs or PEG-HCuSNPs@Au.

REFERENCES

(1). Hwang S; Nam J; Jung S; Song J; Doh H; Kim S, Gold Nanoparticle-Mediated Photothermal Therapy: Current Status and Future Perspective. Nanomedicine (London, U. K.) 2014, 9,2003–2022.

(2). Vankayala R; Hwang KC, Near-Infrared-Light-Activatable Nanomaterial-Mediated Phototheranostic Nanomedicines: An Emerging Paradigm for Cancer Treatment. Adv. Mater 2018, 30, 1706320.

(3). Yang X; Yang MX; Pang B; Vara M; Xia YN, Gold Nanomaterials at Work in Biomedicine. Chem. Rev 2015,115, 10410–10488. [PubMed: 26293344]

(4). Sharifi S; Behzadi S; Laurent S; Laird Forrest M; Stroeve P; Mahmoudi M, Toxicity of Nanomaterials. Chem. Soc. Rev 2012, 41, 2323–2343. [PubMed: 22170510]

(5). Sadauskas E; Danscher G; Stoltenberg M; Vogel U; Larsen A; Wallin H, Protracted Elimination of Gold Nanoparticles from Mouse Liver. Nanomedicine 2009, 5, 162–169. [PubMed: 19217434]

(6). Balasubramanian SK; Jittiwat J; Manikandan J; Ong CN; Yu LE; Ong WY, Biodistribution of Gold Nanoparticles and Gene Expression Changes in the Liver and Spleen after Intravenous Administration in Rats. Biomaterials 2010, 31, 2034–2042. [PubMed: 20044133]

(7). Gharatape A; Salehi R, Recent Progress in Theranostic Applications of Hybrid Gold Nanoparticles. Eur. J. Med. Chem 2017, 138, 221–233. [PubMed: 28668475]

(8). Guo L; Panderi I; Yan DD; Szulak K; Li Y; Chen YT; Ma H; Niesen DB; Seeram N; Ahmed A; Yan B; Pantazatos D; Lu W, A Comparative Study of Hollow Copper Sulfide Nanoparticles and Hollow Gold Nanospheres on Degradability and Toxicity. ACS Nano 2013, 7, 8780–8793. [PubMed: 24053214]

(9). Wang Z; von dem Bussche A; Kabadi PK; Kane AB; Hurt RH, Biological and Environmental Transformations of Copper-Based Nanomaterials. ACS Nano 2013, 7, 8715–8727. [PubMed: 24032665]

(10). Doğan A; Köseoğlu F; Kılıç E, The Stability Constants of Copper (Ii) Complexes with Some A-Amino Acids in Dioxan–Water Mixtures. Anal. Biochem 2001, 295, 237–239. [PubMed: 11488627]

(11). Luza SC; Speisky HC, Liver Copper Storage and Transport During Development: Implications for Cytotoxicity. Am. J. Clin. Nutr 1996, 63, 812S–820S. [PubMed: 8615368]

(12). Polishchuk EV; Concilli M; Iacobacci S; Chesi G; Pastore N; Piccolo P; Paladino S; Baldantoni D; van Ijzendoorn SCD; Chan J; Chang CJ; Amoresano A; Pane F; Pucci P; Tarallo A; Parenti G; Brunetti-Pierri N; Settembre C; Ballabio A; Polishchuk RS, Wilson Disease Protein ATP7B Utilizes Lysosomal Exocytosis to Maintain Copper Homeostasis. Dev. Cell 2014, 29, 686–700. [PubMed: 24909901]

(13). Hasan NM; Gupta A; Polishchuk E; Yu CH; Polishchuk R ; Dmitriev OY; Lutsenko S, Molecular Events Initiating Exit of a Copper-Transporting ATPase ATP7B from the Trans-Golgi Network. J. Biol. Chem 2012, 287, 36041–36050. [PubMed: 22898812]

(14). Nyasae LK; Schell MJ; Hubbard AL, Copper Directs ATP7B to the Apical Domain of Hepatic Cells *Via* Basolateral Endosomes. Traffic 2014, 15, 1344–1365. [PubMed: 25243755]

(15). Tuschl G; Hrach J; Walter Y; Hewitt PG; Mueller SO, Serum-Free Collagen Sandwich Cultures of Adult Rat Hepatocytes Maintain Liver-Like Properties Long Term: A Valuable Model for *in Vitro* Toxicity and Drug-Drug Interaction Studies. Chem.-Biol Interact 2009, 181, 124–137. [PubMed: 19482013]

(16). Keemink J; Oorts M; Annaert P Primary Hepatocytes in Sandwich Culture. In Protocols in In Vitro Hepatocyte Research; Vinken M, Rogiers V, Eds.; Humana Press: New York, 2015; pp 175–188.

(17). Bucci C; Thomsen P; Nicoziani P; McCarthy J; van Deurs B, Rab7: A Key to Lysosome Biogenesis. Mol. Biol. Cell 2000,11, 467–480. [PubMed: 10679007]

(18). Lorinczi E; Tsivkovskii R; Haase W; Bamberg E; Lutsenko S ; Friedrich T, Delivery of the Cu-Transporting ATPase ATP7B to the Plasma Membrane in Xenopus Oocytes. Biochim. Biophys. Acta, Biomembr 2008, 1778, 896–906.

(19). Liu Q; Qian Y; Li P; Zhang S; Liu J; Sun X; Fulham M; Feng D; Huang G; Lu W; Song S, (131)I-Labeled Copper Sulfide-Loaded Microspheres to Treat Hepatic Tumors *Via* Hepatic Artery Embolization. Theranostics 2018, 8, 785–799. [PubMed: 29344306]

(20). Nikoobakht B; El-Sayed MA, Preparation and Growth Mechanism of Gold Nanorods (Nrs) Using Seed-Mediated Growth Method. Chem. Mater 2003, 15, 1957–1962.

(21). Gou LF; Murphy CJ, Fine-Tuning the Shape of Gold Nanorods. Chem. Mater 2005, 17, 3668–3672.

(22). Huang X; Neretina S; El-Sayed MA, Gold Nanorods: From Synthesis and Properties to Biological and Biomedical Applications. Adv. Mater 2009, 21, 4880–4910. [PubMed: 25378252]

(23). Turkevich J; Stevenson PC; Hillier J, A Study of the Nucleation and Growth Processes in the Synthesis of Colloidal Gold. Discuss. Faraday Soc 1951, 11, 55–75.

(24). Deng X; Li K; Cai X; Liu B; Wei Y; Deng K; Xie Z; Wu Z; Ma P; Hou Z; Cheng Z; Lin J, A Hollow-Structured CuS@ Cu_2S@Au Nanohybrid: Synergistically Enhanced Photothermal Efficiency and Photoswitchable Targeting Effect for Cancer Theranostics. Adv. Mater 2017, 29, 1701266.

(25). Liang GH; Jin XD; Qin H; Xing D, Glutathione-Capped, Renal-Clearable Cus Nanodots for Photoacoustic Imaging and Photothermal Therapy. J. Mater. Chem. B 2017, 5, 6366–6375. [PubMed: 32264453]

(26). Kegel V; Deharde D; Pfeiffer E; Zeilinger K; Seehofer D; Damm G, Protocol for Isolation of Primary Human Hepatocytes and Corresponding Major Populations of Non-Parenchymal Liver Cells. J. Visualized Exp 2016, 109, e53069.

(27). More VR; Slitt AL, Alteration of Hepatic but Not Renal Transporter Expression in Diet-Induced Obese Mice. Drug Metab. Dispos 2011, 39, 992–999. [PubMed: 21430232]

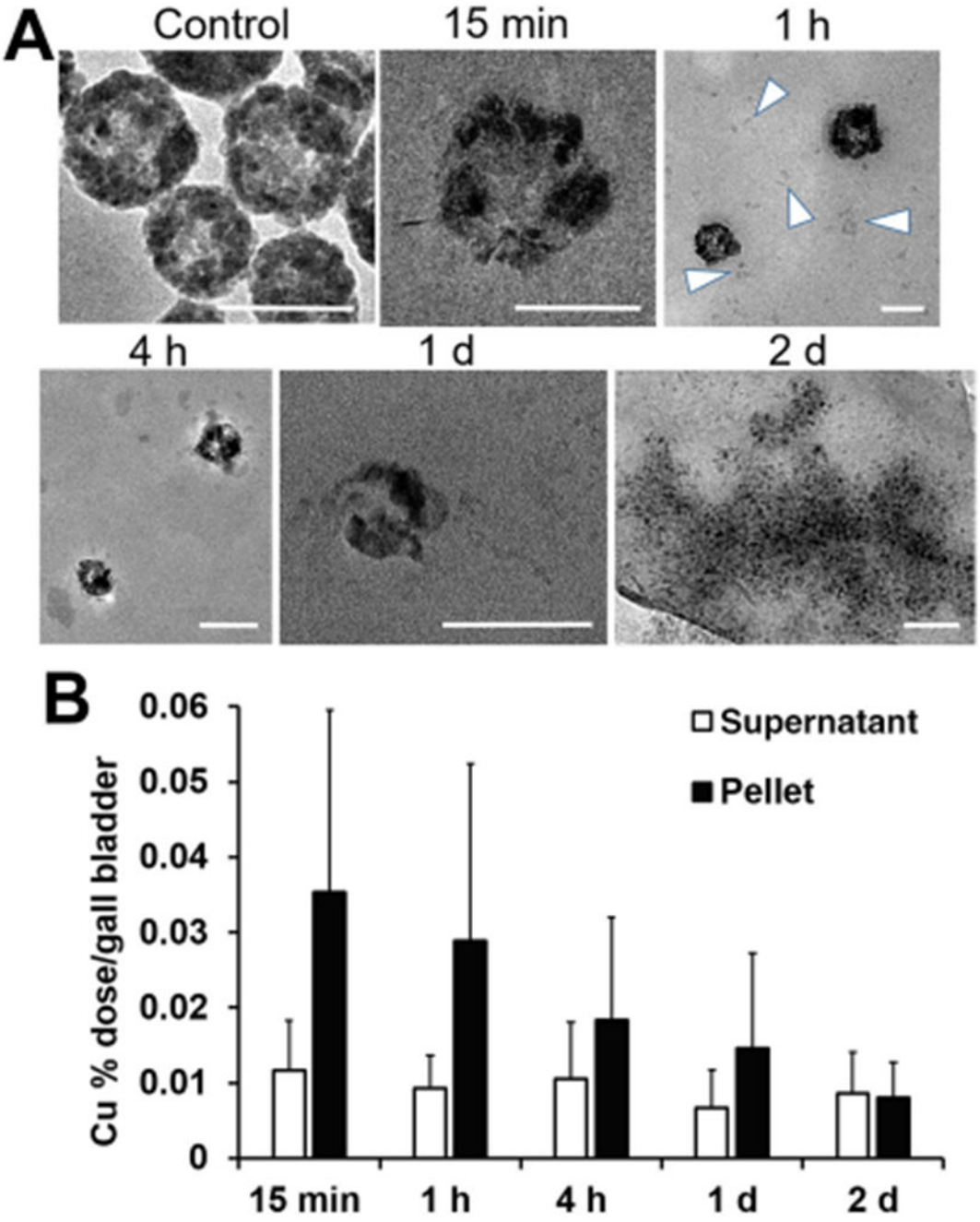

Figure 1.

Fast hepatobiliary excretion of PEG-HCuSNPs. (A) TEM images of PEG-HCuSNPs in bile samples of BALB/c mice at different times following i.v. injection. Control, HCuSNPs in water. Arrowheads, disintegrated CuS nanoparticles. Bars, 100 nm. (B) Cu levels in the supernatant (Cu ions) or pellet (CuS nanoparticles) of gallbladder from BALB/c mice at different times after i.v. injection of PEG-HCuSNPs (20 mg/kg of Cu). Error bars indicate standard deviation (SD) (n = 3–4).

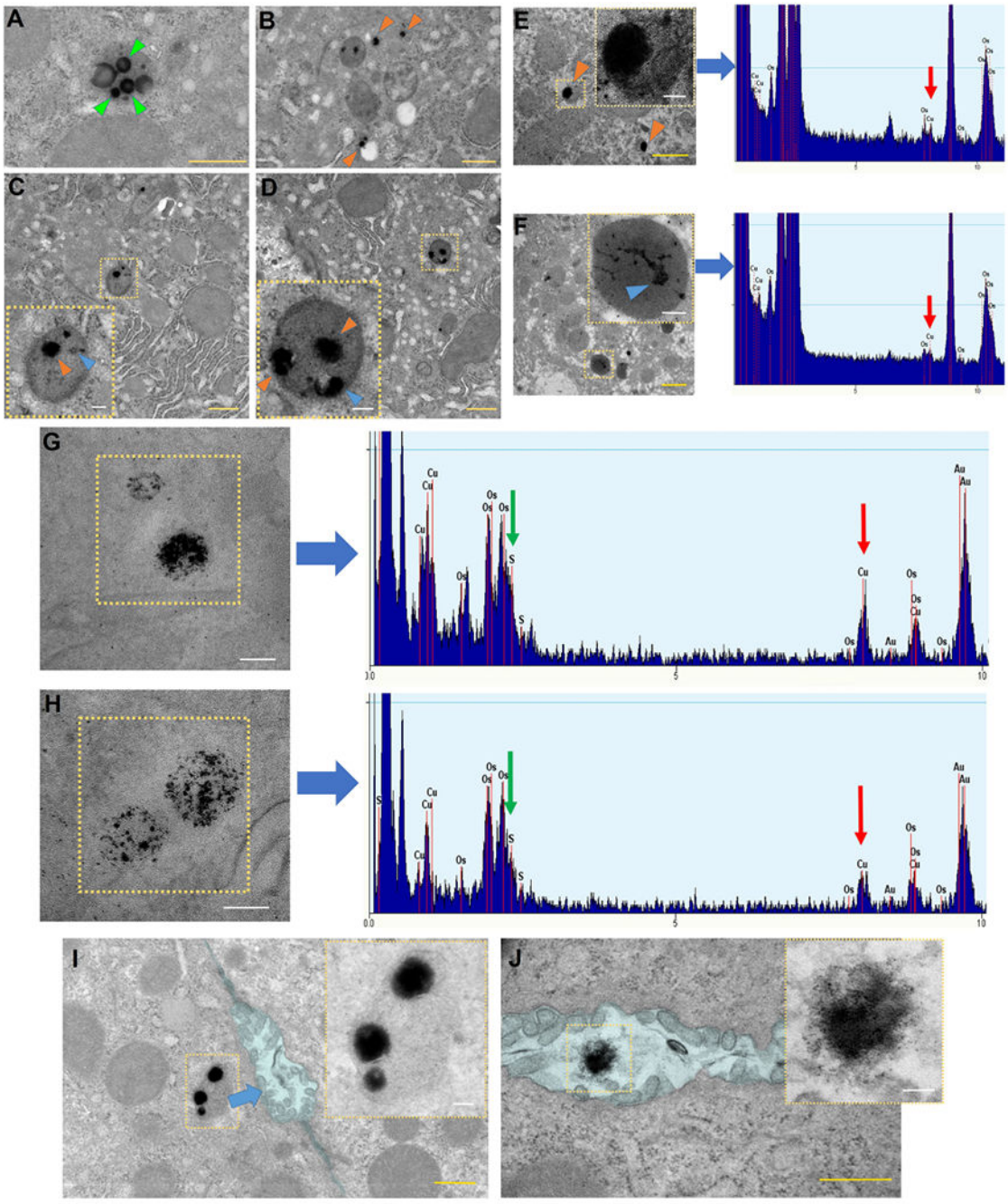

Figure 2.

Distribution of PEG-HCuSNPs in hepatocytes from the liver of mice at 1 h following the injection. (A–D,I,J) TEM images of the ultra-thin-cut liver tissue slices stained with uranyl acetate and lead citrate followed by deposition on the nickel grids. (E,F) TEM images of the liver sections on the molybdenum grids without staining followed by EDS analysis. (G,H) TEM images of the liver sections on the gold grids without staining followed by EDS analysis. Green arrowheads, HCuSNPs; orange arrowheads, CuS nanoparticles with electron-dense structures; blue arrowheads, partially disintegrated HCuSNPs. Red arrows,

Cu element; green arrows, S element; blue arrow, PEG-HCuSNPs-loaded lysosome of hepatocyte trafficking to bile canaliculus. Light cyan, bile canaliculus. Bars in yellow, 500 nm; bars in white, 100 nm.

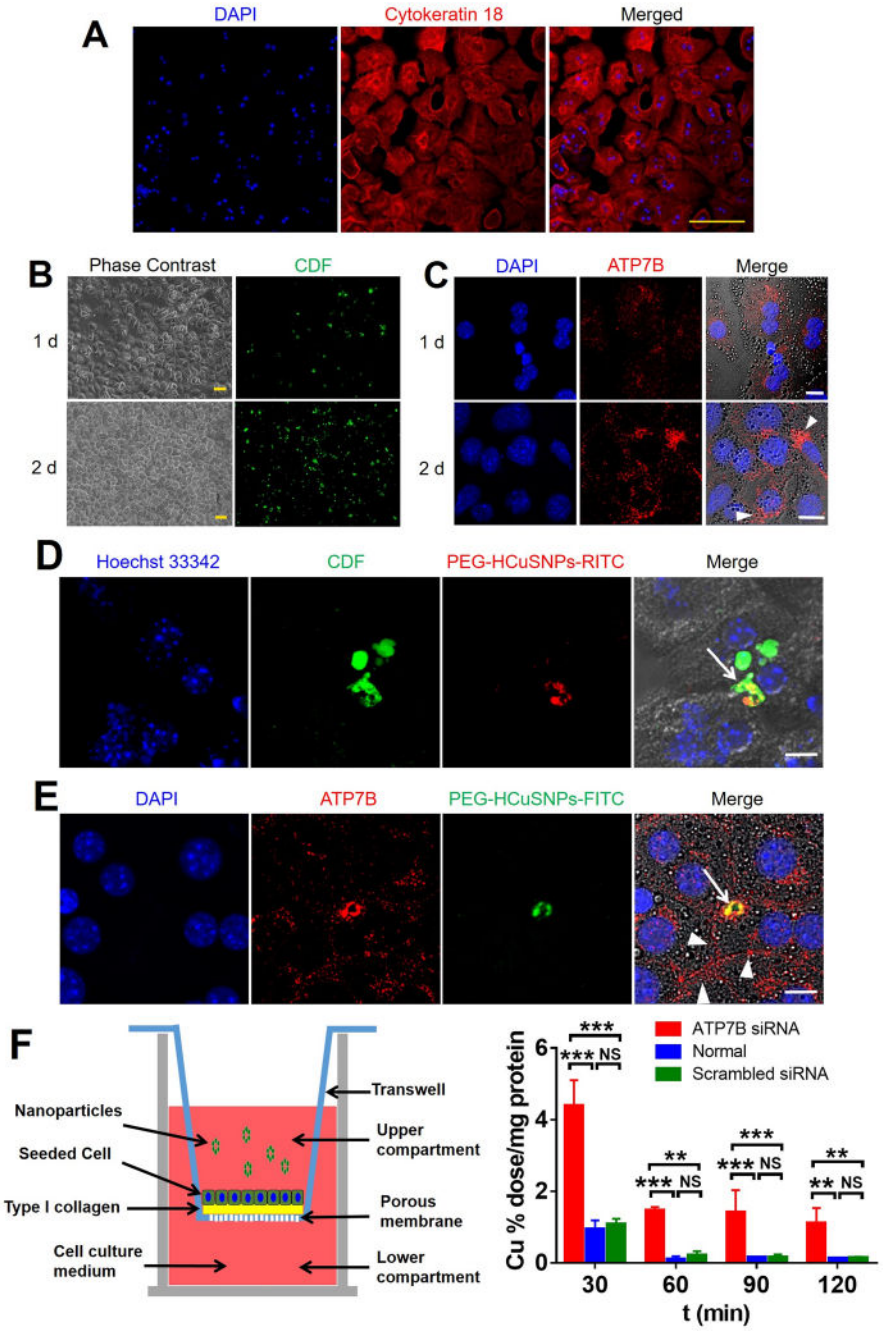

Figure 3.

ATP7B-mediated excretion of PEG-HCuSNPs by the primarily cultured mouse hepatocytes. (A) Immunofluorescence staining of the isolated hepatocytes cultured on collagen-precoated chamber slides for 2 days. (B) Phase contrast and confocal fluorescence imaging of the mouse hepatocytes cultured for 1 or 2 days. The cells were stained with HBSS (with Ca^{2+}/Mg^{2+}) containing 5 μM of CDFDA for 20 min. Green fluorescence, CDF-stained bile canaliculi. (C) Immunofluorescence imaging of ATP7B expression in the primarily isolated hepatocytes cultured for 1 or 2 days. (D,E) Fluorescence micrographs of excretion of PEG-

HCuSNPs by the primarily cultured mouse hepatocytes into bile canaliculi. DAPI, 4′,6-diamidino-2-phenylindole. Arrows, bile canaliculi. (F) Cellular content of Cu particles in the primarily cultured mouse hepatocytes in Transwell transfected with ATP7B siRNA or scrambled siRNA or without treatment (normal). PEG-HCuSNPs were added to the cell culture medium in the upper compartment for 30 min. The cell culture medium of both compartments was then replaced with the fresh medium. Error bars indicate SD ($n = 3$). Bars in yellow, 100 μm; bars in white, 10 μm; $^{**}p < 0.01$, $^{***}p < 0.001$ between the two compared groups. NS, no significant difference between the two compared groups.

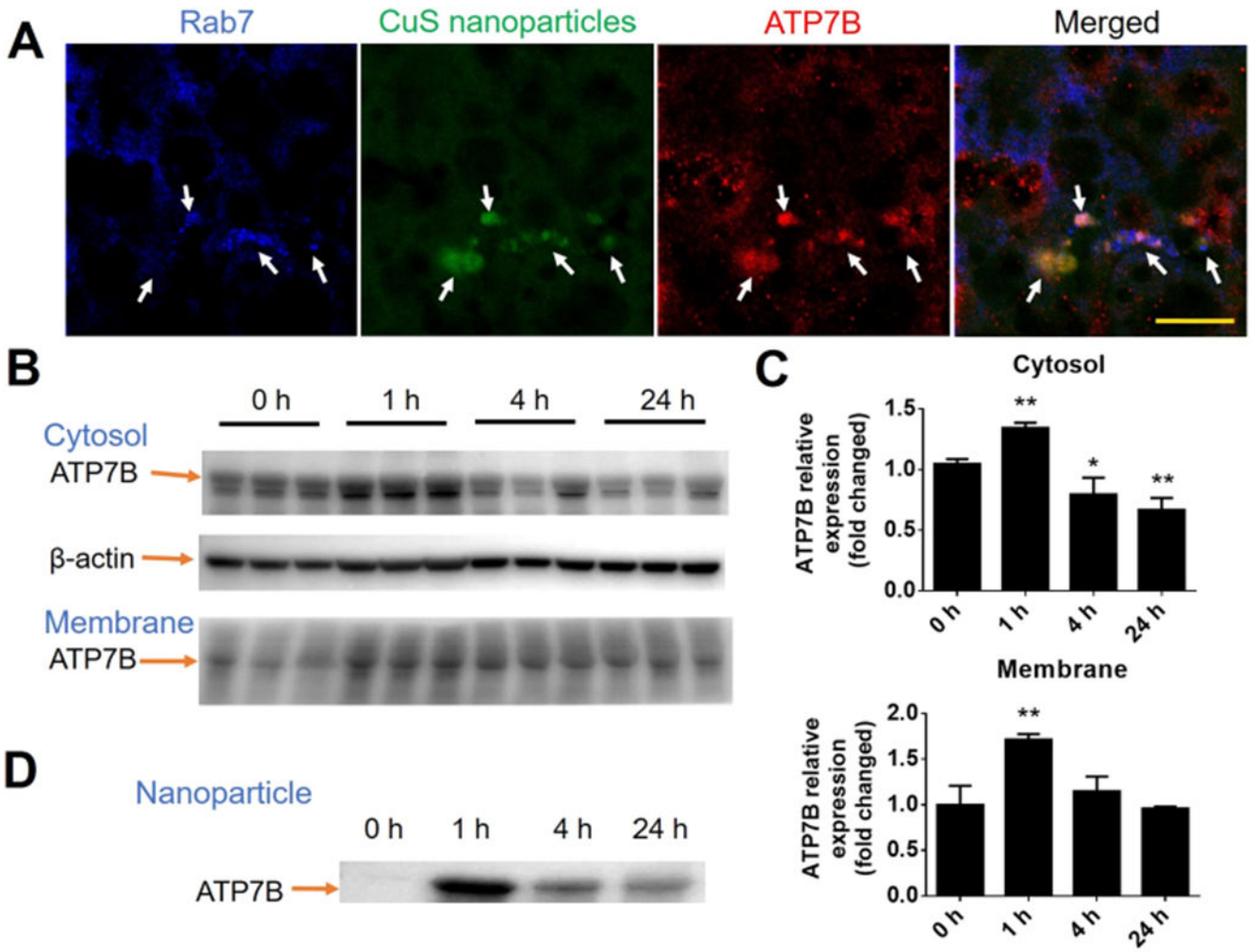

Figure 4.

Trafficking and expression of ATP7B in hepatocytes for the nanoparticle extrusion in response to PEG-HCuSNPs. (A) Immunofluorescence micrographs of the liver from BALB/c mice at 1 h after i.v. injection of PEG-HCuSNPs-FITC. Arrows, colocalization of three fluorescence dyes. Bar, 10 μm. (B) Western blot analysis of ATP7B levels in cytoplasm (top row) or on cytoplasmic membrane (bottom row) of hepatocytes isolated from BALB/c mice at different times after i.v. injection of PEG-HCuSNPs. Three samples of each time point were collected from three mice. "0 h", before injection. (C) Semiquantitative analysis of ATP7B expression in (B). The gray scale intensity of each sample was normalized with that of β-actin expression. ATP7B relative expression represents the ratio of the normalized intensity at different time points to the normalized intensity of the leftmost lane in (B). Error bars indicate SD ($n = 3$); *$p < 0.05$, **$p < 0.01$ significant difference in the ATP7B relative expression at different time vs that at 0 h. (D) Western blot analysis of ATP7B protein adsorbed on CuS nanoparticles in hepatocytes isolated from mice following the injection. One sample at each time point was collected from three mice.

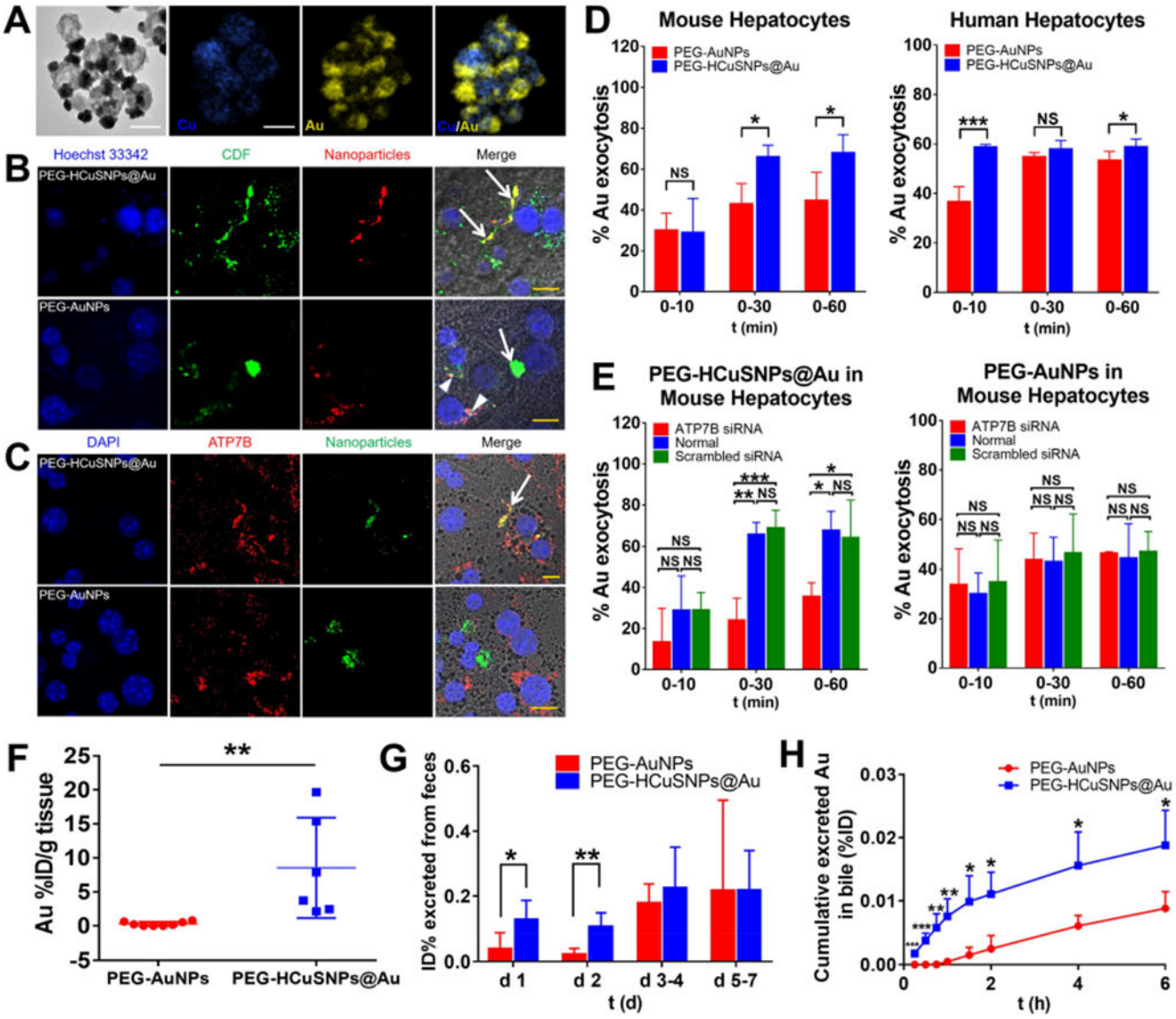

Figure 5.

Facilitated hepatobiliary excretion of PEG-HCuSNPs@Au conjugates. (A) TEM images of PEG-HCuSNPs@Au and EDX mapping the distribution of Cu and Au. Bars, 100 nm. (B,C) Fluorescence micrographs of PEG-HCuSNPs@Au or PEG-AuNPs in primarily cultured mouse hepatocytes at 30 min following incubation. The nanoparticles were labeled with RITC (B) or FITC (C). Arrows, bile canaliculi; arrowheads, intracellular vesicles adjacent to the nuclei. Bars, 10μm. (D) Percent Au exocytosis from the primarily cultured mouse hepatocytes in Transwell (left) or the plated human primary hepatocytes (right) following the 5 min uptake of PEG-HCuSNPs@Au or PEG-AuNPs. The *x*-axis represents the time period of the exocytosis. Error bars indicate SD (n = 3–4). (E) Percent Au exocytosis from the primarily cultured mouse hepatocytes in Transwell transfected with ATP7B siRNA or scrambled siRNA or without treatment (normal). PEG-HCuSNPs@Au (left) or PEG-AuNPs (right) were added to the cell culture medium for 5 min. The cell culture medium was then

replaced with the fresh medium. The *x*-axis represents the time period of the exocytosis. Error bars indicate SD ($n = 3–4$). (F) Quantitative analysis of Au excreted into the gallbladder of mice at 4 h following i.v. injection of PEG-HCuSNPs@Au or PEG-AuNPs (both 20 mg/kg of Au). Error bars indicate SD ($n = 6–8$). (G) Quantitative analysis of Au in feces from mice within different time periods following i.v. injection of PEG-HCuSNPs@Au or PEG-AuNPs (both 20 mg/kg of Au). Error bars indicate SD ($n = 4$). (H) Cumulative Au excretion profile in bile over time from rats following i.v. injection of PEG-HCuSNPs@Au or PEG-AuNPs (both 20 mg/kg of Au). Error bars indicate SD ($n = 3$); $*p < 0.05$, $**p < 0.01$, $***p < 0.001$ between the two compared groups. NS, no significant difference between the two compared groups.

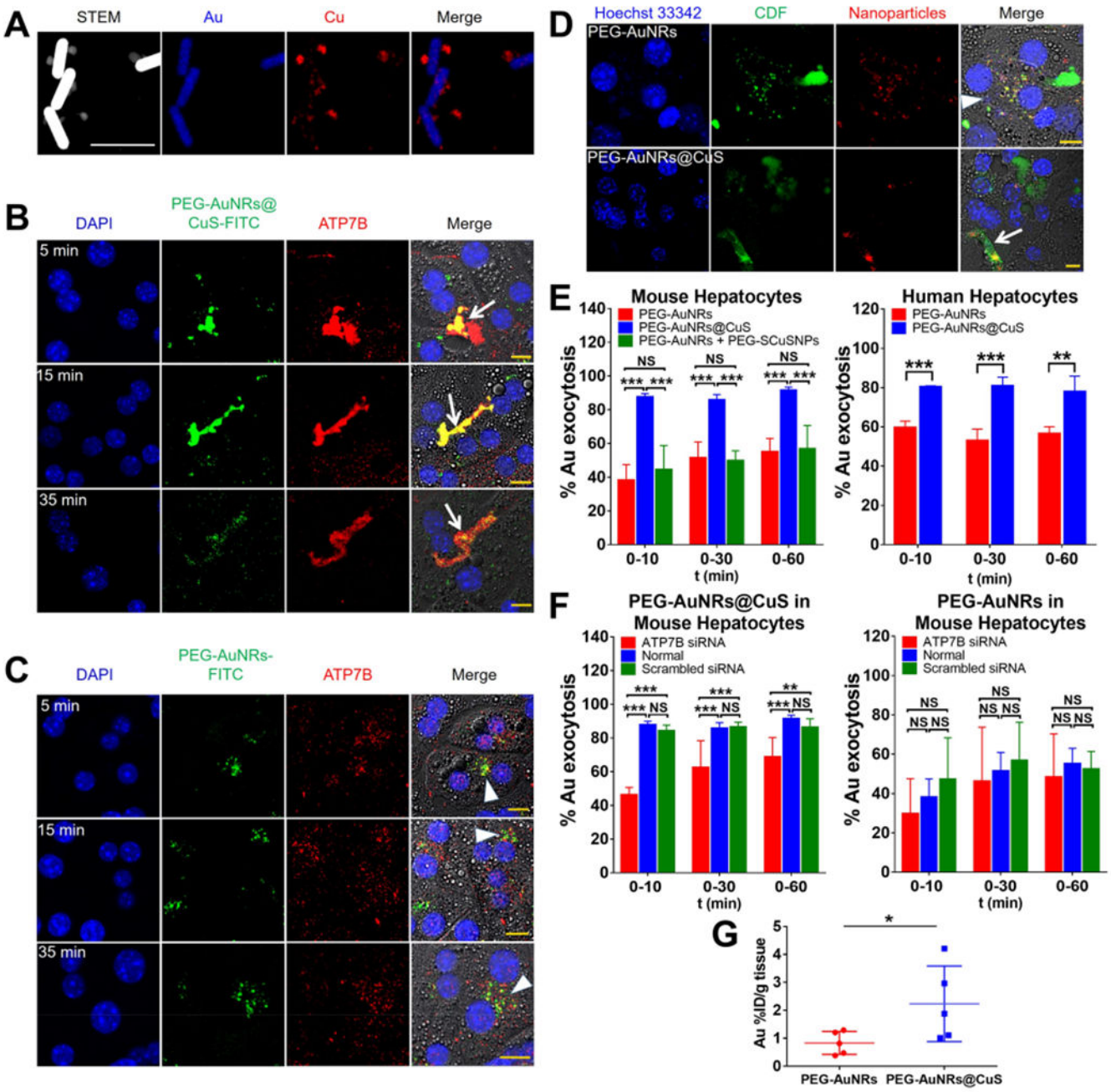

Figure 6.

Facilitated hepatobiliary excretion of PEG-AuNRs@CuS conjugates. (A) STEM/EDX mapping the distribution of Cu and Au of PEG-AuNRs@CuS. (B–D) Fluorescence micrographs of PEG-AuNRs@CuS or PEG-AuNRs in primarily cultured mouse hepatocytes following incubation with the nanoparticles for different times (B,C) or 30 min (D). The nanoparticles were labeled with FITC (B,C) or RITC (D). Arrows, bile canaliculi; arrowheads, intracellular vesicles adjacent to the nuclei. (E) Percent Au exocytosis from the primarily cultured mouse hepatocytes in Transwell (left) or the plated human primary hepatocytes (right) following the 5 min uptake of PEG-AuNRs@CuS or PEG-AuNRs. PEG-

AuNRs + PEG-SCuSNPs group, mouse hepatocytes were treated with the mixture of PEG-AuNRs and PEG-SCuSNPs with the same Au/Cu ratio as that of PEG-AuNRs@CuS. The *x*-axis represents the time period of the exocytosis. Error bars indicate SD ($n = 3–4$). (F) Percent Au exocytosis from the primarily cultured mouse hepatocytes in Transwell transfected with ATP7B siRNA or scrambled siRNA or without treatment (normal). PEG-AuNRs@CuS (left) or PEG-AuNRs (right) were added to the cell culture medium for 5 min. The cell culture medium was then replaced with the fresh medium. The *x*-axis represents the time period of the exocytosis. Error bars indicate SD ($n = 3–4$). (G) Quantitative analysis of Au excreted into bile of mice at 4 h following i.v. injection of PEG-AuNRs@CuS or PEG-AuNRs (both 20 mg/kg of Au). Error bars indicate SD ($n = 5$); $^{*}p < 0.05$, $^{**}p < 0.01$, $^{***}p < 0.001$ between the two compared groups. NS, no significant difference between the two compared groups. Bars in yellow, 10 μm; bars in white, 50 nm.

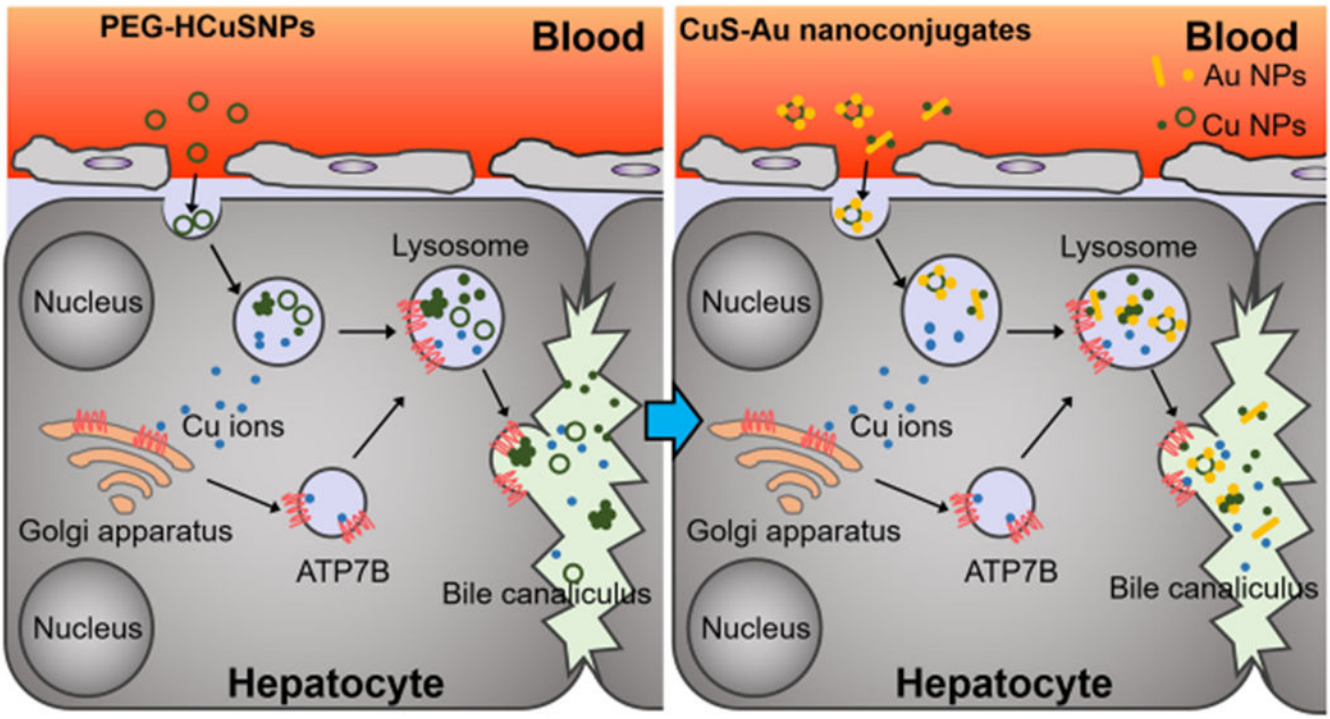

Scheme 1.

Illustration Showing Trafficking Pathways of Hepatobiliary Excretion of PEG-HCuSNPs (Left) and CuS–Au Nanoconjugates (Right) by Hepatocytes Following Intravenous Administration.